

# Union of Intersections (UoI) for Interpretable Data Driven Discovery and Prediction

Kristofer E. Bouchard\* Alejandro F. Bujan† Farbod Roosta-Khorasani‡  
 Shashanka Ubaru§ Prabhat¶ Antoine M. Snijders|| Jian-Hua Mao\*\*  
 Edward F. Chang†† Michael W. Mahoney†† Sharmodeep Bhattacharyya§§

## Abstract

The increasing size and complexity of scientific data could dramatically enhance discovery and prediction for basic scientific applications. Realizing this potential, however, requires novel statistical analysis methods that are both interpretable and predictive. We introduce Union of Intersections (UoI), a flexible, modular, and scalable framework for enhanced model selection and estimation. Methods based on UoI perform model selection and model estimation through intersection and union operations, respectively. We show that UoI-based methods achieve low-variance and nearly unbiased estimation of a small number of interpretable features, while maintaining high-quality prediction accuracy. We perform extensive numerical investigation to evaluate a UoI algorithm ( $UoI_{Lasso}$ ) on synthetic and real data. In doing so, we demonstrate the extraction of interpretable functional networks from human electrophysiology recordings as well as accurate prediction of phenotypes from genotype-phenotype data with reduced features. We also show (with the  $UoI_{L1Logistic}$  and  $UoI_{CUR}$  variants of the basic framework) improved prediction parsimony for classification and matrix factorization on several benchmark biomedical

---

\*Biological Systems and Engineering Division, Lawrence Berkeley National Laboratory; Computational Research Division, Lawrence Berkeley National Laboratory; Redwood Center for Theoretical Neuroscience, University of California at Berkeley; Kavli Institute for Fundamental Neuroscience, University of California at San Francisco; Email: kebouchard@lbl.gov

†Redwood Center for Theoretical Neuroscience, University of California at Berkeley; Email: afbujan@gmail.com

‡International Computer Science Institute; Department of Statistics, University of California at Berkeley; Email: farbod@icsi.berkeley.edu

§Department of Computer Science and Engineering, University of Minnesota-Twin Cities; Email: ubaru001@umn.edu

¶National Energy Research Super Computing, Lawrence Berkeley National Laboratory; Email: prabhat@lbl.gov

||Biological Systems and Engineering Division, Lawrence Berkeley National Laboratory; Email: AMSnijders@lbl.gov

\*\*Biological Systems and Engineering Division, Lawrence Berkeley National Laboratory; Email: jhmao@lbl.gov

††UCSF Epilepsy Center, University of California at San Francisco; Department of Neurological Surgery, University of California at San Francisco; Email: Edward.Chang@ucsf.edu

††International Computer Science Institute; Department of Statistics, University of California at Berkeley; Email: mmahoney@stat.berkeley.edu

§§Department of Statistics, Oregon State University; Email: bhattach@science.oregonstate.edu

data sets. These results suggest that methods based on the UoI framework could improve interpretation and prediction in data-driven discovery across scientific fields.

## 1 Introduction

A central goal of data-driven science is to identify a small number of features (i.e., predictor variables;  $X$  in Fig. 1(a)) that generate a response variable of interest ( $y$  in Fig. 1(a)) and then to estimate the relative contributions of these features as the parameters in the generative process relating the predictor variables to the response variable (Fig. 1(a)). A common characteristic of many modern massive data sets is that they have a large number of features (i.e., high-dimensional data), while also exhibiting a high degree of sparsity and/or redundancy [3, 40, 20]. That is, while formally high-dimensional, most of the useful information in the data features for tasks such as reconstruction, regression, and classification can be restricted or compressed into a much smaller number of important features. In regression and classification, it is common to employ sparsity-inducing regularization to attempt to achieve simultaneously two related but quite different goals: to identify the features important for prediction (i.e., model selection) and to estimate the associated model parameters (i.e., model estimation) [3, 40]. For example, the Lasso algorithm in linear regression uses  $L_1$ -regularization to penalize the total magnitude of model parameters, and this often results in feature compression by setting some parameters exactly to zero [39] (See Fig. 1(a), pure white elements in right-hand vectors, emphasized by  $\times$ ). It is well known that this type of regularization implies a prior assumption about the distribution of the parameter (e.g.,  $L_1$ -regularization implicitly assumes a Laplacian prior distribution) [24]. However, strong sparsity-inducing regularization, which is common when there are many more potential features than data samples (i.e., the so-called small  $n/p$  regime) can severely hinder the *interpretation* of model parameters (Fig. 1(a), indicated by less saturated colors between top and bottom vectors on right hand side). For example, while sparsity may be achieved, incorrect features may be chosen and parameters estimates may be biased. In addition, it can impede model selection and estimation when the true model distribution deviates from the assumed distribution [3, 17]. This may not matter for prediction quality, but it clearly has negative consequences for *interpretability*, an admittedly not completely-well-defined property of algorithms that is crucial in many scientific applications [13]. In this context, *interpretability* reflects the degree to which an algorithm returns a small number of physically meaningful features with unbiased estimates of their contributions.

On the other hand, another common characteristic of many state of the art methods is to combine several related models for a given task. In statistical data analysis, this is often formalized by so-called ensemble methods, which improve prediction accuracy by combining parameter estimates [24]. In particular, by combining several different models, ensemble methods often include more features to predict the response variables, and thus the number of data features is expanded relative to the

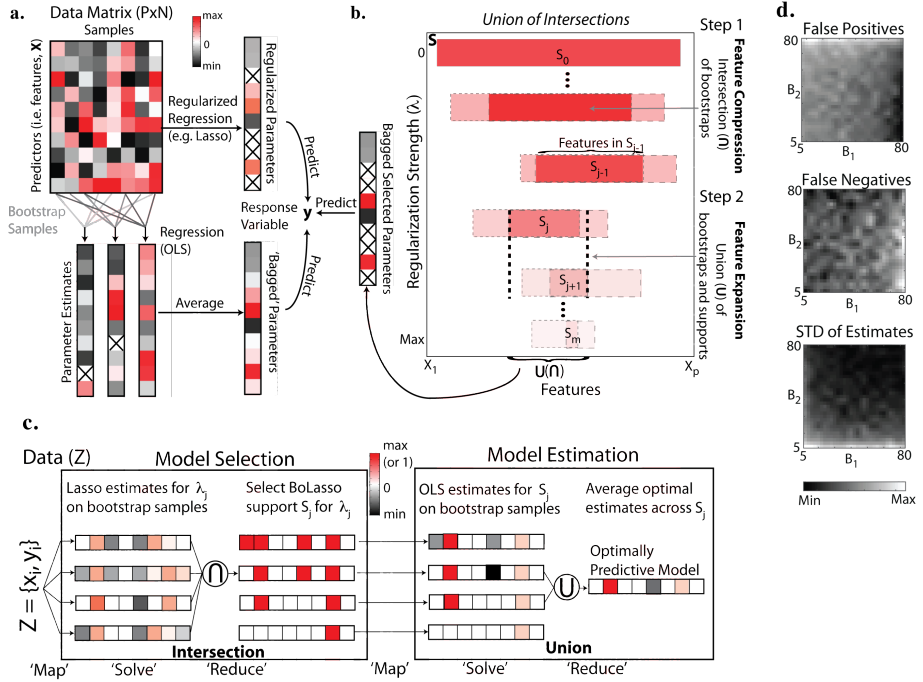


Figure 1: **The basic UoI framework.** (a) Schematic of regularization and ensemble methods for regression. (b) Schematic of the Union of Intersections (UoI) framework. (c) A data-distributed version of the  $UoI_{Lasso}$  algorithm. (d) Dependence of false positive, false negatives, and estimation variability on number of bootstraps in selection ( $B_1$ ) and estimation ( $B_2$ ) modules.

individuals in the ensemble. For example, estimating an ensemble of model parameters by randomly resampling the data many times (e.g., bootstrapping) and then averaging the parameter estimates (e.g., bagging) can yield improved prediction accuracy by reducing estimation variability [9, 24] (See Fig. 1(a), bottom). However, by averaging estimates from a large ensemble, this process often results in many non-zero parameters, which can hinder interpretability and the identification of the true model support (compare top and bottom vectors on right hand side of Fig. 1(a)). Taken together, these observations suggest that explicit and more precise control of feature compression and expansion may result in an algorithm with improved interpretative and predictive properties.

In this paper, we introduce Union of Intersections (UoI), a flexible, modular, and scalable framework to enhance both the identification of features (model selection) as well as the estimation of the contributions of these features (model estimation). We have found that the UoI framework permits us to explore the interpretability-predictivity trade-off space, without imposing an explicit prior on the model distribution, and without formulating a non-convex problem, thereby often leading to improved interpretability and prediction. Ideally, data analysis methods in many scientific applications should be selective (only features that influence the response variable are selected),

accurate (estimated parameters in the model are as close to the true value as possible), predictive (allowing prediction of the response variable), stable (e.g., the variability of the estimated parameters is small), and scalable (able to return an answer in a reasonable amount of time on very large data sets) [37, 3, 31, 17]. We show empirically that UoI-based methods can simultaneously achieve these goals. We primarily demonstrate the power of UoI-based methods in the context of sparse linear regression ( $UoI_{Lasso}$ ), as it is the canonical statistical/machine learning problem, it is theoretically tractable, and it is widely used in virtually every field of scientific inquiry. However, our framework is very general, and we demonstrate this by extending UoI to classification ( $UoI_{L1Logistic}$ ) and matrix factorization ( $UoICUR$ ) problems. While our main focus is on neuroscience (broadly speaking) applications, our results also highlight the power of UoI across a broad range of synthetic and real scientific data sets.

## 2 Union of Intersections (UoI)

For concreteness, we consider an application of UoI in the context of the linear regression. Specifically, we consider the problem of estimating the parameters  $\beta \in \mathbb{R}^p$  that map a  $p$ -dimensional vector of predictor variables  $x \in \mathbb{R}^p$  to the observation variable  $y \in \mathbb{R}$ , when there are  $n$  paired samples of  $x$  and  $y$  corrupted by i.i.d Gaussian noise:

$$y = \beta^T x + \varepsilon, \quad (1)$$

where  $\varepsilon \stackrel{iid}{\sim} N(0, \sigma^2)$  for each sample. When the true  $\beta$  is thought to be sparse (i.e., in the  $L_0$ -norm sense), then an estimate of  $\beta$  (call it  $\hat{\beta}$ ) can be found by solving a constrained optimization problem of the form:

$$\hat{\beta} \in \operatorname{argmin}_{\beta \in \mathbb{R}^p} \sum_{i=1}^n (y_i - \beta x_i)^2 + \lambda R(\beta). \quad (2)$$

Here,  $R(\beta)$  is a regularization term that typically penalizes the overall magnitude of the parameter vector  $\beta$  (e.g.,  $R(\beta) = \|\beta\|_1$  is the target of the Lasso algorithm).

**The Basic UoI Framework.** The key mathematical idea underlying UoI is to perform model selection through intersection (compressive) operations and model estimation through union (expansive) operations, in that order. This is schematized in Fig. 1(b), which plots a hypothetical range of selected features ( $x_1 : x_p$ , abscissa) for different values of the regularization parameter ( $\lambda$ , ordinate), and a more detailed description of this is provided in the Appendix. In particular, UoI first performs feature compression (Fig. 1(b), Step 1) through intersection operations (intersection of supports across bootstrap samples) to construct a family ( $S$ ) of candidate model supports (Fig. 1(b), e.g.,  $S_{j-1}$ , opaque red region is intersection of abutting pink regions). UoI then performs feature expansion (Fig. 1(b), Step 2) through a union of (potentially) different model supports: for each bootstrap sample, the best model estimates (across different supports) is chosen, and then a new

model is generated by averaging the estimates (i.e., taking the union) across bootstrap samples (Fig. 1(b), dashed vertical black line indicates the union of features from  $S_j$  and  $S_{j+1}$ ). Both feature compression and expansion are performed across all regularization strengths. In UoI, feature compression via intersections and feature expansion via unions are balanced to maximize prediction accuracy of the sparsely estimated model parameters for the response variable  $y$ .

**Innovations in Union of Intersections.** UoI has three central innovations: (1) calculate model supports ( $S_j$ ) using an intersection operation for a range of regularization parameters (increases in  $\lambda$  shrink all values  $\hat{\beta}$  towards 0), efficiently constructing a family of potential model supports  $\{S : S_j \in S_{j-k}, \text{ for } k \text{ sufficiently large}\}$ ; (2) use a novel form of *model averaging* in the union step to directly optimize prediction accuracy (this can be thought of as a hybrid of bagging [9] and boosting [36]); and (3) combine pure model selection using an intersection operation with model selection/estimation using a union operation in that order (which controls both false negatives and false positives in model selection). Together, these innovations often lead to better selection, estimation and prediction accuracy. Importantly, this is done without explicitly imposing a prior on the distribution of parameter values, and without formulating a non-convex optimization problem.

**The  $UoI_{Lasso}$  Algorithm.** Since the basic UoI framework, as described in Fig. 1(c), has two main computational modules—one for model selection, and one for model estimation—UoI is a framework into which many existing algorithms can be inserted. Here, for simplicity, we primarily demonstrate UoI in the context of linear regression in the  $UoI_{Lasso}$  algorithm, although we also apply it to classification with the  $UoI_{L1Logistic}$  algorithm as well as matrix factorization with the  $UoI_{CUR}$  algorithm. (See the Appendix for pseudo-code for the  $UoI_{Lasso}$  algorithm.)  $UoI_{Lasso}$  expands on the BoLasso method for the model selection module [1], and it performs a novel *model averaging* in the estimation module based on averaging ordinary least squares (OLS) estimates with potentially different model supports.  $UoI_{Lasso}$  (and UoI in general) has a high degree of natural algorithmic parallelism that we have exploited in a distributed Python-MPI implementation. (Fig. 1(c) schematizes a simplified distributed implementation of the algorithm, and see the Appendix for more details.) This parallelized  $UoI_{Lasso}$  algorithm uses distribution of bootstrap data samples and regularization parameters (in *Map*) for independent computations involving convex optimizations (Lasso and OLS, in *Solve*), and it then combines results (in *Reduce*) with intersection operations (model selection module) and union operations (model estimation module). By solving independent convex optimization problems (e.g., Lasso, OLS) with distributed data resampling, our  $UoI_{Lasso}$  algorithm efficiently constructs a family of model supports, and it then averages nearly unbiased model estimates, potentially with different supports, to maximize prediction accuracy while minimizing the number of features to aid interpretability.

### 3 Results

We start with a discussion of the basic methodological setup. The main statistical properties are discussed numerically in Section 3.2. The rest of this section describes our extensive empirical evaluation on real and synthetic data of several variants of the basic UoI framework.

#### 3.1 Methods

All numerical results used 100 random sub-samplings with replacement of 80-10-10 cross-validation to estimate model parameters (80%), choose optimal meta-parameters (e.g.,  $\lambda$ , 10%), and determine prediction quality (10%). Below,  $\beta$  denotes the values of the true model parameters,  $\hat{\beta}$  denotes the estimated values of the model parameters from some algorithm (e.g.,  $UoI_{Lasso}$ ),  $S_\beta$  is the support of the true model (i.e., the set of non-zero parameter indices), and  $S_{\hat{\beta}}$  is the support of the estimated model. We calculated several metrics of model selection, model estimation, and prediction accuracy. (1) Selection accuracy (set overlap):  $1 - \frac{|S_{\hat{\beta}} \Delta S_\beta|}{|S_{\hat{\beta}}|_0 + |S_\beta|_0}$ , where,  $\Delta$  is the symmetric set difference operator. This metric ranges in  $[0, 1]$ , taking a value of 0 if  $S_\beta$  and  $S_{\hat{\beta}}$  have no elements in common, and taking a value of 1 if and only if they are identical. (2) Estimation error (r.m.s):  $\sqrt{\frac{1}{p} \sum (\beta_i - \hat{\beta}_i)^2}$ . (3) Estimation variability (parameter variance):  $E[\hat{\beta}^2] - (E[\hat{\beta}])^2$ . (4) Prediction accuracy ( $R^2$ ):  $\frac{\sum (y_i - \hat{y}_i)^2}{\sum (y_i - E[y])^2}$ . (5) Prediction parsimony (BIC):  $n \log(\frac{1}{n-1} \sum_{i=1}^n (y_i - \hat{y}_i)^2) + \|\hat{\beta}\|_0 \log(n)$ . For the experimental data, as the true model size is unknown, the selection ratio ( $\frac{\|\hat{\beta}\|_0}{p}$ ) is a measure of the overall size of the estimated model relative to the total number of parameters. For the classification task using  $UoI_{L1Logistic}$ , BIC was calculated as:  $-2 \log \ell + S_{\hat{\beta}} \log N$ , where  $\ell$  is the log-likelihood on the validation set. For the matrix factorization task using  $UoI_{CUR}$ , reconstruction accuracy was the Frobenius norm of the difference between the data matrix  $A$  and the low-rank approximation matrix  $A'$  constructed from  $A(:, c)$ , the reduced column matrix of  $A$ :  $\|A - A'\|_F$ , where  $c$  is the set of  $k$  selected columns.

#### 3.2 Model Selection and Stability: Explicit Control of False Positives, False Negatives, and Estimate Stability

Due to the form of the basic UoI framework, we can control both false negative and false positive discoveries, as well as the stability of the estimates. For any regularized regression method like in (2), a decrease in the penalization parameter ( $\lambda$ ) tends to increase the number of false positives, and an increase in  $\lambda$  tends to increase in false negatives. Preliminary analysis of the UoI framework shows that, for false positives, a large number of bootstrap resamples in the intersection step ( $B_1$ ) produces an increase in the probability of getting no false positive discoveries, while an increase in the number of bootstraps in the union step ( $B_2$ ) leads to a decrease in the probability of getting no false positives. Conversely, for false negatives, a large number of bootstrap resamples in the union

step ( $B_2$ ) produces an increase in the probability of no false negative discoveries, while an increase in the number of bootstraps in the intersection step ( $B_1$ ) leads to a decrease in the probability of no false negatives. Also, a large number of bootstrap samples in union step ( $B_2$ ) gives a more stable estimate. These properties were confirmed numerically for  $UoI_{Lasso}$  and are displayed in Fig. 1(d), which plots the average normalized false negatives, false positives, and standard deviation of model estimates from running  $UoI_{Lasso}$ , with ranges of  $B_1$  and  $B_2$  on four different models. Thus, the relative values of  $B_1$  and  $B_2$  express the fundamental balance between the two basic operations of intersection (which compresses the feature space) and union (which expands the feature space). Model selection through intersection often excludes true parameters (i.e., false negatives), and, conversely, model estimation using unions often includes erroneous parameters (i.e., false positives). By using stochastic resampling, combined with model selection through intersections, followed by model estimation through unions, UoI permits us to mitigate the feature inclusion/exclusion inherent in either operation. Essentially, the limitations of selection by intersection are counteracted by the union of estimates, and vice versa.

### 3.3 $UoI_{Lasso}$ has Superior Performance on Simulated Data Sets

To explore the performance of the  $UoI_{Lasso}$  algorithm, we have performed extensive numerical investigations on simulated data sets, where we can control key properties of the data. There are a large number of algorithms available for linear regression, and we picked some of the most popular algorithms (e.g., Lasso), as well as more uncommon, but more powerful algorithms (e.g., SCAD, a non-convex method). Specifically, we compared  $UoI_{Lasso}$  to five other model selection/estimation methods: Ridge, Lasso, SCAD, BoATS, and debiased Lasso [24, 39, 17, 5, 4, 26]. Note that BoATS and debiased Lasso are both two-stage methods. We examined performance of these algorithms across a variety of underlying distributions of model parameters, degrees of sparsity, and noise levels. Across all algorithms examined, we found that  $UoI_{Lasso}$  (Fig. 2, black) generally resulted in very high selection accuracy (Fig. 2(c), right) with parameter estimates with low error (Fig. 2(c), center-right), leading to the best prediction accuracy (Fig. 2(c), center-left) and prediction parsimony (Fig. 2(c), left). In addition, it was very robust to differences in underlying parameter distribution, degree of sparsity, and magnitude of noise. (See the Appendix for more details.)

### 3.4 $UoI_{Lasso}$ in Neuroscience: Sparse Functional Networks from Human Neural Recordings and Parsimonious Prediction from Genetic and Phenotypic Data

We sought to determine if the enhanced selection and estimation properties of  $UoI_{Lasso}$  also improved its utility as a tool for data-driven discovery in complex, diverse neuroscience data sets. Neurobiology seeks to understand the brain across multiple spatio-temporal scales, from molecules-to-minds.

**Figure 2**

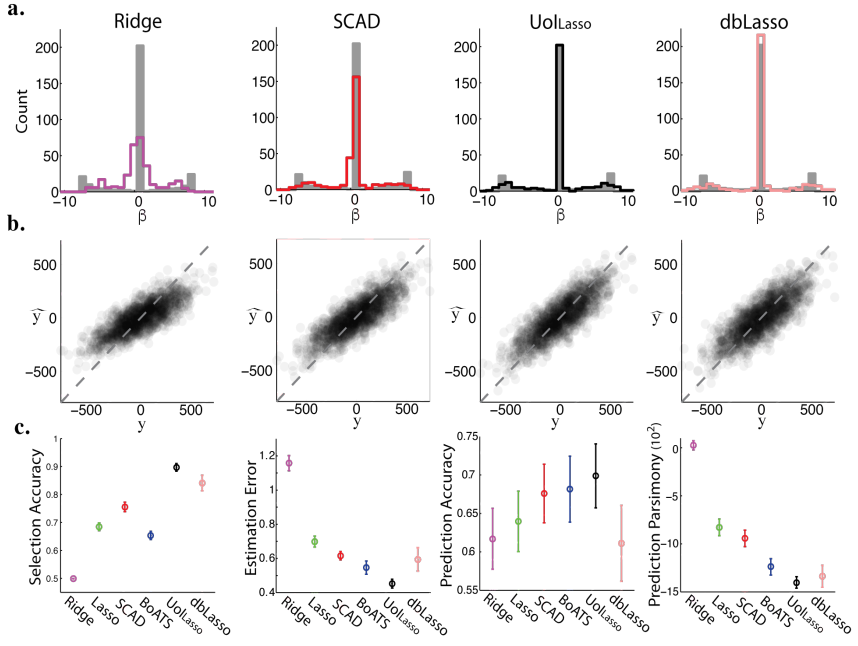


Figure 2: **Range of observed results, in comparison with existing algorithms.** (a) True  $\beta$  distribution (grey histograms) and estimated values (colored lines). (b) Scatter plot of true and estimated values of observation variable on held-out samples. (c) Metrics of algorithm performance.

We first tackled the problem of graph formation from multi-electrode ( $p = 86$  electrodes) neural recordings taken directly from the surface of the human brain during speech production ( $n = 45$  trials each). See [7] for details. That is, the goal was to construct sparse neuroscientifically-meaningful graphs for further downstream analysis. To estimate functional connectivity, we calculated partial correlation graphs. The model was estimated independently for each electrode, and we compared the results of graphs estimated by  $UoILasso$  to the graphs estimated by SCAD. In Fig. 3(a)-(b), we display the networks derived from recordings during the production of /b/ while speaking /ba/. We found that the  $UoILasso$  network (Fig. 3(a)) was much sparser than the SCAD network (Fig. 3(b)). Furthermore, the network extracted by  $UoILasso$  contained electrodes in the lip (dorsal vSMC), jaw (central vSMC), and larynx (ventral vSMC) regions, accurately reflecting the articulators engaged in the production of /b/ (Fig. 3(c)) [7]. The SCAD network (Fig. 3(d)) did not have any of these properties. This highlights the improved power of  $UoILasso$  to extract sparse graphs with functionally meaningful features relative to even some non-convex methods.

We calculated connectivity graphs during the production of 9 consonant-vowel syllables. Fig. 3(e) displays a summary of prediction accuracy for  $UoILasso$  networks (red) and SCAD networks (black) as a function of time. The average relative prediction accuracy (compared to baseline times) for the

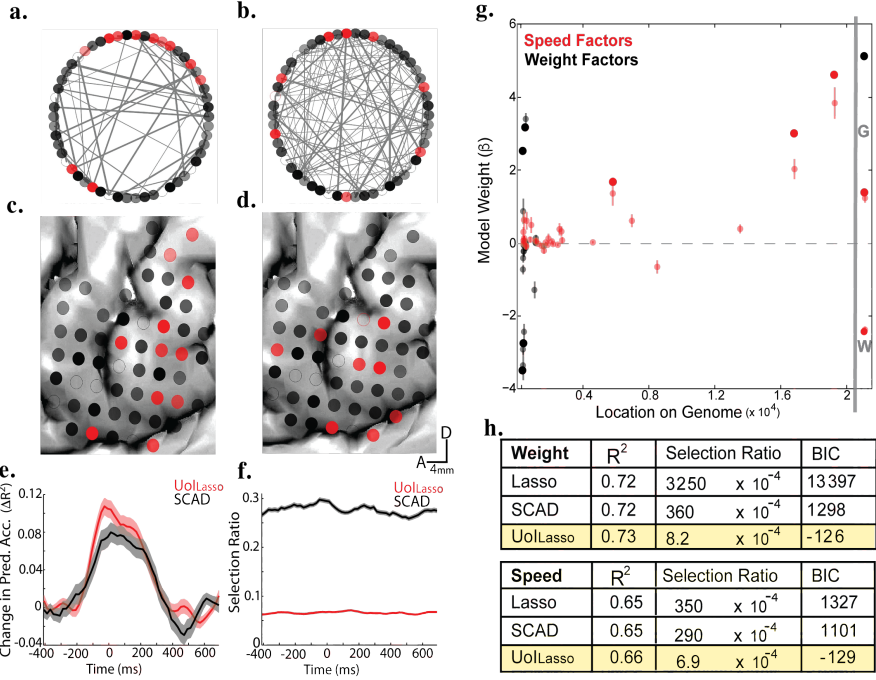


Figure 3: **Application of UoI to neuroscience and genetics data.** (a)-(f): Functional connectivity networks from ECoG recordings during speech production. (g)-(h): Parsimonious prediction of complex phenotypes from genotype and phenotype data.

$UoI_{Lasso}$  network was generally greater during the time of peak phoneme encoding [ $T = -100:200$ ] compared to the SCAD network. Fig. 3(f) plots the time course of the parameter selection ratio for the  $UoI_{Lasso}$  network (red) and SCAD network (black). The  $UoI_{Lasso}$  network was consistently  $\sim 5\times$  sparser than the SCAD network. These results demonstrate that  $UoI_{Lasso}$  extracts sparser graphs from noisy neural signals with a modest increase in prediction accuracy compared to SCAD.

We next investigated whether  $UoI_{Lasso}$  would improve the identification of a small number of highly predictive features from genotype-phenotype data. To do so, we analyzed data from  $n = 365$  mice (173 female, 192 male) that are part of the genetically diverse Collaborative Cross cohort. We analyzed single-nucleotide polymorphisms (SNPs) from across the entire genome of each mouse ( $p = 11,563$  SNPs). For each animal, we measured two continuous, quantitative phenotypes: weight and behavioral performance on the rotarod task (see [30] for details). We focused on predicting these phenotypes from a small number of genotype-phenotype features. We found that  $UoI_{Lasso}$  identified and estimated a small number of features that were sufficient to explain large amounts of variability in these complex behavioral and physiological phenotypes. Fig. 3(g) displays the non-zero values estimated for the different features (e.g., location of loci on the genome) contributing to the weight (black) and speed (red) phenotype. Here, non-opaque points correspond to the mean  $\pm$  s.d. across

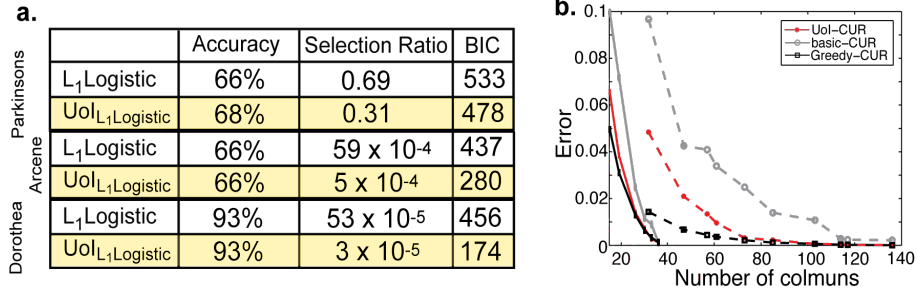


Figure 4: **Extension of UoI to classification and matrix decomposition.** (a) UoI for classification ( $UoI_{L_1}L_1$ Logistic). (b) UoI for matrix decomposition ( $UoI_{CUR}$ ); solid and dashed lines are for PAH and dashed SORCH data sets, respectively.

cross-validation samples, while the opaque points are the medians. Importantly, for both speed and weight phenotypes, we confirmed that several identified predictor features had been reported in the literature, though by different studies, e.g., genes coding for Kif1b, Rrm2b/Ubr5, and Dloc2. (See the Appendix for more details.) Accurate prediction of phenotypic variability with a small number of factors was a unique property of models found by  $UoI_{Lasso}$ . For both weight and rotorod performance, models fit by  $UoI_{Lasso}$  had marginally increased prediction accuracy compared to other methods (+1%), but they did so with far fewer parameters (lower selection ratios). This results in prediction parsimony (BIC) that was several orders of magnitude better (Fig. 3(h)). Together, these results demonstrate that  $UoI_{Lasso}$  can identify a small number of genetic/physiological factors that are highly predictive of complex physiological and behavioral phenotypes.

### 3.5 $UoI_{L_1}L_1$ Logistic and $UoI_{CUR}$ : Application of UoI to Classification and Matrix Decomposition

As noted, UoI is a framework into which other methods can be inserted. While we have primarily demonstrated UoI in the context of linear regression, it is much more general than that. To illustrate this, we implemented a classification algorithm ( $UoI_{L_1}L_1$ Logistic) and matrix decomposition algorithm ( $UoI_{CUR}$ ), and we compared them to the base methods on several data sets (see Appendix for details). In classification, UoI resulted in either equal or improved prediction accuracy with 2x-10x fewer parameters for a variety of biomedical classification tasks (Fig. 4(a)). For matrix decomposition (in this case, column subset selection), for a given dimensionality, UoI resulted in reconstruction errors that were consistently lower than the base method (BasicCUR), and quickly approached an unscalable greedy algorithm (GreedyCUR) for two genetics data sets (Fig. 4(b)). In both cases, UoI improved the prediction parsimony relative to the base (classification or decomposition) method.

## 4 Discussion

UoI-based methods leverage stochastic data resampling and a range of sparsity-inducing regularization parameters/dimensions to build families of potential features, and they then average nearly unbiased parameter estimates of selected features to maximize predictive accuracy. Thus, UoI separates model selection with intersection operations from model estimation with union operations: the limitations of selection by intersection are counteracted by the union of estimates, and vice versa. Stochastic data resampling can be viewed as a perturbation of the data, and UoI efficiently identifies and robustly estimates features that are stable to these perturbations. A unique property of UoI-based methods is the ability to control both false positives and false negatives. Increasing the number of bootstraps in the selection module ( $B_1$ ) increases the amount of feature compression (primary controller of false positives), while increasing the number of bootstraps in the estimation module ( $B_2$ ) increases feature expansion (primary controller of false negatives), and we observe this empirically. Thus, neither should be too large, and their relative values express the balance between feature compression and expansion. This tension is seen in many places in machine learning and data analysis: local nearest neighbor methods vs. global latent factor models; local spectral methods that tend to expand due to their diffusion-based properties vs. flow-based methods that tend to contract; and sparse  $L_1$  vs. dense  $L_2$  penalties/priors more generally. Interestingly, an analogous balance of compressive and expansive forces contributes to neural learning algorithms based on Hebbian synaptic plasticity [6]. Our results highlight how revisiting popular methods in light of new data science demands can lead to still further-improved methods, and they suggest several directions for theoretical and empirical work.

## References

- [1] F. R. Bach. Bolasso: model consistent Lasso estimation through the bootstrap. In *Proceedings of the 25th international conference on Machine learning*, pages 33–40, 2008.
- [2] R. M. Bell and Y. Koren. Lessons from the Netflix prize challenge. *SIGKDD Explorations*, 9(2):75–79, December 2007.
- [3] P. Bickel and B. Li. Regularization in statistics. *TEST*, 15(2):271–344, 2006.
- [4] K. E. Bouchard. Bootstrapped adaptive threshold selection for statistical model selection and estimation. Technical report, 2015. Preprint: arXiv:1505.03511.
- [5] K. E. Bouchard and E. F. Chang. Control of spoken vowel acoustics and the influence of phonetic context in human speech sensorimotor cortex. *Journal of Neuroscience*, 34(38):12662–12677, 2014.

- [6] K. E. Bouchard, S. Ganguli, and M. S. Brainard. Role of the site of synaptic competition and the balance of learning forces for Hebbian encoding of probabilistic Markov sequences. *Frontiers in Computational Neuroscience*, 9(92), 2015.
- [7] K. E. Bouchard, N. Mesgarani, K. Johnson, and E. F. Chang. Functional organization of human sensorimotor cortex for speech articulation. *Nature*, 495(7441):327–332, 2013.
- [8] C. Boutsidis, M. W. Mahoney, and P. Drineas. An improved approximation algorithm for the column subset selection problem. In *Proceedings of the 20th Annual ACM-SIAM Symposium on Discrete Algorithms*, pages 968–977, 2009.
- [9] L. Breiman. Bagging predictors. *Machine Learning*, 24(2):123–140, 1996.
- [10] L. Breiman. Random forests. *Machine Learning*, 45(1):5–32, 2001.
- [11] C. S. Carlson, M. A. Eberle, L. Kruglyak, and D. A. Nickerson. Mapping complex disease loci in whole-genome association studies. *Nature*, 429(6990):446–452, 2004.
- [12] C. Cortes and V. Vapnik. Support-vector networks. *Machine Learning*, 20(3):273–297, 1995.
- [13] National Research Council. *Frontiers in Massive Data Analysis*. The National Academies Press, Washington, D. C., 2013.
- [14] P. Dayan and L. F. Abbott. *Theoretical neuroscience: computational and mathematical modeling of neural systems*. MIT Press, Cambridge, 2001.
- [15] P. Drineas, M. Magdon-Ismail, M. W. Mahoney, and D. P. Woodruff. Fast approximation of matrix coherence and statistical leverage. *Journal of Machine Learning Research*, 13:3475–3506, 2012.
- [16] P. Drineas, M. W. Mahoney, and S. Muthukrishnan. Relative-error CUR matrix decompositions. *SIAM Journal on Matrix Analysis and Applications*, 30:844–881, 2008.
- [17] J. Fan and R. Li. Variable selection via nonconcave penalized likelihood and its oracle properties. *Journal of the American Statistical Association*, 96(456):1348–1360, 2001.
- [18] R. A. Fisher. The correlation between relatives on the supposition of Mendelian inheritance. *Philosophical Transactions of the Royal Society of Edinburgh*, 52:399–433, 1918.
- [19] J. Freeman, N. Vladimirov, T. Kawashima, Y. Mu, N. J. Sofroniew, D. V. Bennett, J. Rosen, C.-T. Yang, L. L. Looger, and M. B. Ahrens. Mapping brain activity at scale with cluster computing. *Nature Methods*, 11:941–950, 2014.

- [20] S. Ganguli and H. Sompolinsky. 2012. *Annual Review of Neuroscience*, 35(1):485–508, Compressed Sensing, Sparsity, and Dimensionality in Neuronal Information Processing and Data Analysis.
- [21] R. A. Gibbs et al. The international HapMap project. *Nature*, 426(6968):789–796, 2003.
- [22] A. Gittens, A. Devarakonda, E. Racah, M. Ringenburg, L. Gerhardt, J. Kottaalam, J. Liu, K. Maschhoff, S. Canon, J. Chhugani, P. Sharma, J. Yang, J. Demmel, J. Harrell, V. Krishnamurthy, M. W. Mahoney, and Prabhat. Matrix factorization at scale: a comparison of scientific data analytics in Spark and C+MPI using three case studies. Technical report, 2016. Preprint: arXiv:1607.01335.
- [23] D. B. Goldstein. Common genetic variation and human traits. *New England Journal of Medicine*, 360(17):696–1698, 2009.
- [24] T. Hastie, R. Tibshirani, and J. Friedman. *The Elements of Statistical Learning*. Springer-Verlag, New York, 2003.
- [25] H. Hotelling. Relations between two sets of variates. *Biometrika*, 28:321–377, 1936.
- [26] A. Javanmard and A. Montanari. Confidence intervals and hypothesis testing for high-dimensional regression. *Journal of Machine Learning Research*, 15:2869–2909, 2014.
- [27] E. S. Lander and L. Kruglyak. Genetic dissection of complex traits - guidelines for interpreting and reporting linkage results. *Nature Genetics*, 11(3):241–247, 1995.
- [28] M. W. Mahoney. *Randomized algorithms for matrices and data*. Foundations and Trends in Machine Learning. NOW Publishers, Boston, 2011.
- [29] M. W. Mahoney and P. Drineas. CUR matrix decompositions for improved data analysis. *Proc. Natl. Acad. Sci. USA*, 106:697–702, 2009.
- [30] J.-H. Mao, S. A. Langley, Y. Huang, M. Hang, K. E. Bouchard, S. E. Celniker, J. B. Brown, J. K. Jansson, G. H. Karpen, and A. M. Snijders. Identification of genetic factors that modify motor performance and body weight using collaborative cross mice. *Scientific Reports*, 5:16247, 2015.
- [31] V. Marx. Biology: The big challenges of big data. *Nature*, 498(7453):255–260, 2013.
- [32] N. Meinshausen and P. Bühlmann. Stability selection. *Journal of the Royal Statistical Society, Series B*, 72(4):417–473, 2010.

- [33] M. V. Osier, K.-H. Cheung, J. R. Kidd, A. J. Pakstis, P. L. Miller, and K. K. Kidd. ALFRED: an allele frequency database for diverse populations and DNA polymorphisms—an update. *Nucleic acids research*, 29(1):317–319, 2001.
- [34] P. Paschou, M. W. Mahoney, A. Javed, J. R. Kidd, A. J. Pakstis, S. Gu, K. K. Kidd, and P. Drineas. Intra- and interpopulation genotype reconstruction from tagging SNPs. *Genome Research*, 17(1):96–107, 2007.
- [35] J. W. Pillow, J. Shlens, L. Paninski, A. Shera, A. M. Litke, E. J. Chichilnisky, and E. P. Simoncelli. Spatio-temporal correlations and visual signalling in a complete neuronal population. *Nature*, 454(7207):995–999, 2008.
- [36] R. E. Schapire and Y. Freund. *Boosting: Foundations and Algorithms*. MIT Press, Cambridge, MA, 2012.
- [37] T. J. Sejnowski, P. S. Churchland, and J. A. Movshon. Putting big data to good use in neuroscience. *Nature Neuroscience*, 17(11):1440–1441, 2014.
- [38] I. H. Stevenson et al. Functional connectivity and tuning curves in populations of simultaneously recorded neurons. *PLoS Computational Biology*, 8(11):e1002775, 2012.
- [39] R. Tibshirani. Regression shrinkage and selection via the lasso. *Journal of the Royal Statistical Society: Series B*, 58(1):267–288, 1996.
- [40] M. J. Wainwright. Structured regularizers for high-dimensional problems: Statistical and computational issues. *Annual Review of Statistics and Its Application*, 1:233–253, 2014.
- [41] D. Welter, J. MacArthur, J. Morales, T. Burdett, P. Hall, H. Junkins, A. Klemm, P. Flicek, T. Manolio, L. Hindorff, and H. Parkinson. The NHGRI GWAS Catalog, a curated resource of SNP-trait associations. *Nucleic acids research*, 42(Database issue):D1001–6, 2014.
- [42] A. R. Wood et al. Defining the role of common variation in the genomic and biological architecture of adult human height. *Nature Genetics*, 46(11):1173–1186, 2014.

## A Additional Material

In this appendix section, we will provide additional information about the UoI method. We will start in Section A.1 with an extended introduction for scientific data. Then, in Section A.2, we provide pseudo-code for  $UoI_{Lasso}$ ; in Section A.3, we discuss scaling issues; in Section A.4, we discuss expanded results for the simulated data example; in Section A.5, we discuss simulated data across different parameter distributions and levels of sparsity; in Section A.6, we discuss simulated data across different noise magnitudes; in Section A.7, we discuss  $UoI_{L1Logistic}$  for classification problems; and in Section A.8, we discuss  $UoI_{CUR}$  for applying matrix decompositions to genetics data. We conclude in Section A.9 with a brief additional discussion and conclusion.

### A.1 Extended Introduction for Scientific Examples

An important aspect of the use of machine learning and data analysis techniques in scientific applications—as opposed to internet, social media, and related applications—is that scientific researchers often implicitly or explicitly interpret the output of their data analysis tools as reflecting the true state of nature. For example, in neuroscience, one often wants to understand how neural activity (e.g., action potentials, calcium transients, cortical field potentials, etc.) is mapped to features of the external world (e.g., sounds or movement), or to features of the brain itself (e.g., the activity of other brain areas) [14]. A common approach to this is to formulate the mapping as a parametric model and then estimate the model parameters from noisy data. In addition to providing predictive capabilities, such model parameters can also provide insight into neural representations, functional connectivity, and population dynamics [35, 38, 5]. Indeed, this insight into the underlying neuroscience is typically at least as important as the predictive quality of the model. Likewise, in molecular biology and medicine, recent advances have allowed for the proliferation of low-cost whole-genome mapping, paving the way for large-scale genome wide association studies (GWAS) [41]. The relationship between genetic variations and observed phenotypes can be estimated from a parametric model [18, 11, 42]. Here, researchers may be interested in methods that allow for the identification of low-penetrance genes that are present at high frequency in a population, as these are likely the major genetic components associated with predisposition to disease risk and other physiological and behavioral phenotypes [27, 23]. Because the molecules encoded by the genes are often used to guide future experiments or drug development, identifying a small number of genetic factors that are highly predictive is critical to accelerate basic discovery and targets for next generation therapeutics. These and other examples [13] illustrate that the prediction-versus-interpretation data analysis needs of the scientific community are not well aligned with the needs of the Internet and social media industries that are forcing functions for the development of many machine learning and data analysis methods.

## A.2 Pseudo-code for the $UoI_{Lasso}$ Algorithm

Here, we provide pseudo-code for a  $UoI_{Lasso}$  algorithm.

**Algorithm:**  $UoI_{Lasso}$  Input: data  $(X, Y) \in \mathbb{R}^{n \times (p+1)}$ ;

vector of regularization parameters  $\lambda \in \mathbb{R}^q$ ;

number of bootstraps  $B_1$  and  $B_2$ ;

### % Model Selection

for  $k=1$  to  $B_1$  do

Generate bootstrap sample  $T^k = (X_T^k, Y_T^k)$

for  $\lambda_j \in \lambda$  do

Compute Lasso estimate  ${}^j\hat{\beta}^k$  from  $T^k$

Compute support  $S_j^k = \{i\}$  s.t.  ${}^j\hat{\beta}_i^k \neq 0$

end for

end for

for  $j=1$  to  $q$  do

Compute BoLasso support for  $\lambda_j$ :  $S_j = \bigcap_{k=1}^{B_1} S_j^k$

end for

### % Model Estimation

for  $k=1$  to  $B_2$  do

Generate bootstrap samples for cross-validation:

training  $T^k = (X_T^k, Y_T^k)$

evaluation  $E^k = (X_E^k, Y_E^k)$

for  $j=1$  to  $q$  do

Compute OLS estimate  $\hat{\beta}_{S_j}^k$  from  $T^k$

Compute loss on  $E^k$ :  $L(\hat{\beta}_{S_j}^k, E^k)$

end for

Compute best model for each bootstrap sample:

$\hat{\beta}_S^k = \underset{\hat{\beta}_{S_j}^k}{\operatorname{argmin}} L(\hat{\beta}_{S_j}^k, E^k)$

end for

Compute bagged model estimate  $\hat{\beta}^* = \frac{1}{B_2} \sum_{k=1}^{B_2} \hat{\beta}_S^k$

Return:  $\hat{\beta}^*$

As described in the main text, UoI is a framework that includes performing complementary unions and intersections of a basic underlying method. When applied to  $L_1$ -regularized  $L_2$  regression, we obtain the  $UoI_{Lasso}$  algorithm. This pseudo-code implements a serial version of the  $UoI_{Lasso}$  algorithm. The algorithm uses the BoLasso method for the model selection through the intersection module, and bagged ordinary least squares regression for the the estimation through the union module. This algorithm is described serially, but, as schematized in Fig. 1(c), this algorithm has a great deal of natural parallelism, involving independent calculations across different bootstrap samples ( $B_1$  and  $B_2$ ) and values of the regularization parameter ( $\lambda$ ), which occur for both the selection and estimation modules. Of course, further algorithmic parallelization can be achieved by distributing the computations required for solving the Lasso and OLS convex-optimization steps, using, e.g., the Alternating Directions Method of Multiplies (ADMM). Even for linear regression, other methods could be used for the selection module (e.g., SCAD, stability selection, etc.), though keeping the estimation module as an un-regularized method should be maintained. When other base algorithms are used, e.g., a logistic classifier or a CUR matrix decomposition, then other variants of the basic UoI framework, such as  $UoI_{L1Logistic}$  and  $UoICUR$  (that are described below and in the main text), are obtained.

### A.3 Scaling of the $UoI_{Lasso}$ Algorithm

$UoI_{Lasso}$  (and UoI in general) has a high degree of natural algorithmic parallelism that we have exploited in a distributed Python-MPI implementation. (See Section 3.1 also.) To assess the scalability of the algorithm, we carried out a series of scaling computations with data sets of different sizes; and, in Fig. 5, we present a summary of the performance between a serial and a distributed implementation of  $UoI_{Lasso}$ . We used the computational runtime and the input-output (IO) time as performance indicators. We used artificially generated data sets with sizes that ranged from 400 bytes to 40 gigabytes, therefore spanning 5 orders of magnitude in size, and we performed computations on a supercomputer (NERSC at LBNL), as described in Section 3.1. Fig. 5(a) shows the computational runtime for the distributed and the serial program compared across data set sizes, as indicated by the gray scale color and the legend. All data points in Fig 5(a) lie well above the identity line shown as a diagonal gray dashed line, which indicates that runtime was in all cases notably lower for the distributed version of  $UoI_{Lasso}$ . This improvement in runtime increased with the data set size: the best-fit line to the (log-log) data had a slope of 1.19 and y-intercept of 2.13. This indicates a general improvement of approximately two-orders of magnitude (y-intercept), and that improvements get better for larger data sets (slope greater than 1). The computational runtime is also shown in Fig. 5(b) with pink and gray bars, and in addition this plot includes the IO time shown with red and black bars for the parallel and serial versions of  $UoI_{Lasso}$ , respectively. We found that even though IO time was slightly larger in the parallel version for small data sets, IO operations

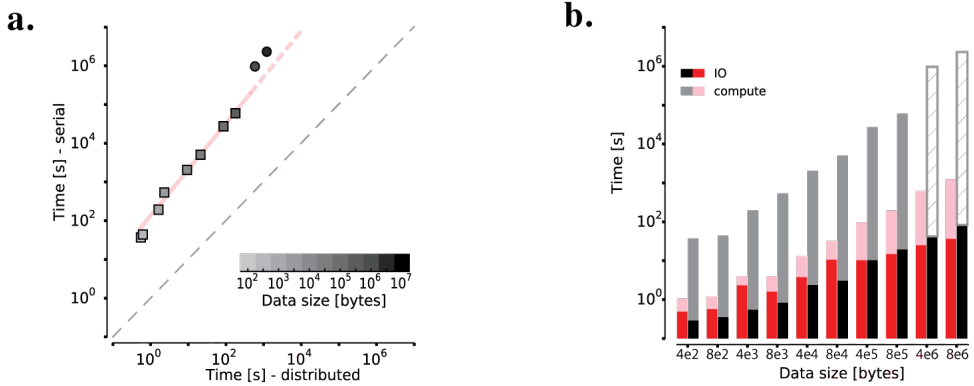


Figure 5: **Efficient and scalable implementation of  $UoILasso$  on distributed computing systems.** (a) Comparison of computational runtime between serial and distributed  $UoILasso$ , as a function of the data set size. Gray-scale: size of the design matrix in bytes (legend). Circular markers: computational runtime of serial  $UoILasso$  was estimated using a single iteration. Square markers: actual data points. Red line: linear fit to the actual (log-log) data (squares). Grey dashed line is unity. (b) Computational runtime and data IO time for serial (grey/black) and distributed (pink/red)  $UoILasso$  as a function of data set size (x-axis). Hatched bars: estimated runtime time using a single iteration.

benefited from the distributed implementation when large datasets were analyzed. Overall, these results show a good scalability, in parallel settings, of the basic UoI framework, illustrating its potential applicability to very large-scale data sets.

#### A.4 $UoILasso$ Outperforms Other Methods: Expanded Results for Simulated Data

Here, we extend the results from the example simulation that were presented in Fig. 2 in the main text. To remind the reader, we compared  $UoILasso$  (black) to five other model estimation methods: Ridge (purple), Lasso (green), SCAD (red), BoATS (blue), and debiased Lasso (pink). We quantified several metrics of both model recovery (i.e., selection accuracy and estimation error) and prediction quality (accuracy:  $R^2$ ; parsimony: Bayesian Information Criterion). The expanded results presented in Fig. 6 are for a simulated data set generated from a model with parameters distributed as the grey histogram in Fig. 6(b). In particular, there were  $n = 1200$  examples with observation variables ( $y$ ) generated from Eqn. (1), with  $p = 300$  total parameters ( $n/p = 4$ ),  $k = 100$  non-zero parameters (sparsity:  $1 - k/p = 0.66$ ) that were symmetrically distributed with exponentially increasing frequency as a function of parameter magnitude, and noise magnitude of  $\sigma^2 = 0.2 \times \sum_j |\beta_j|$ . We took statistics of the metrics across 100 randomized cross-validation samples of the data.

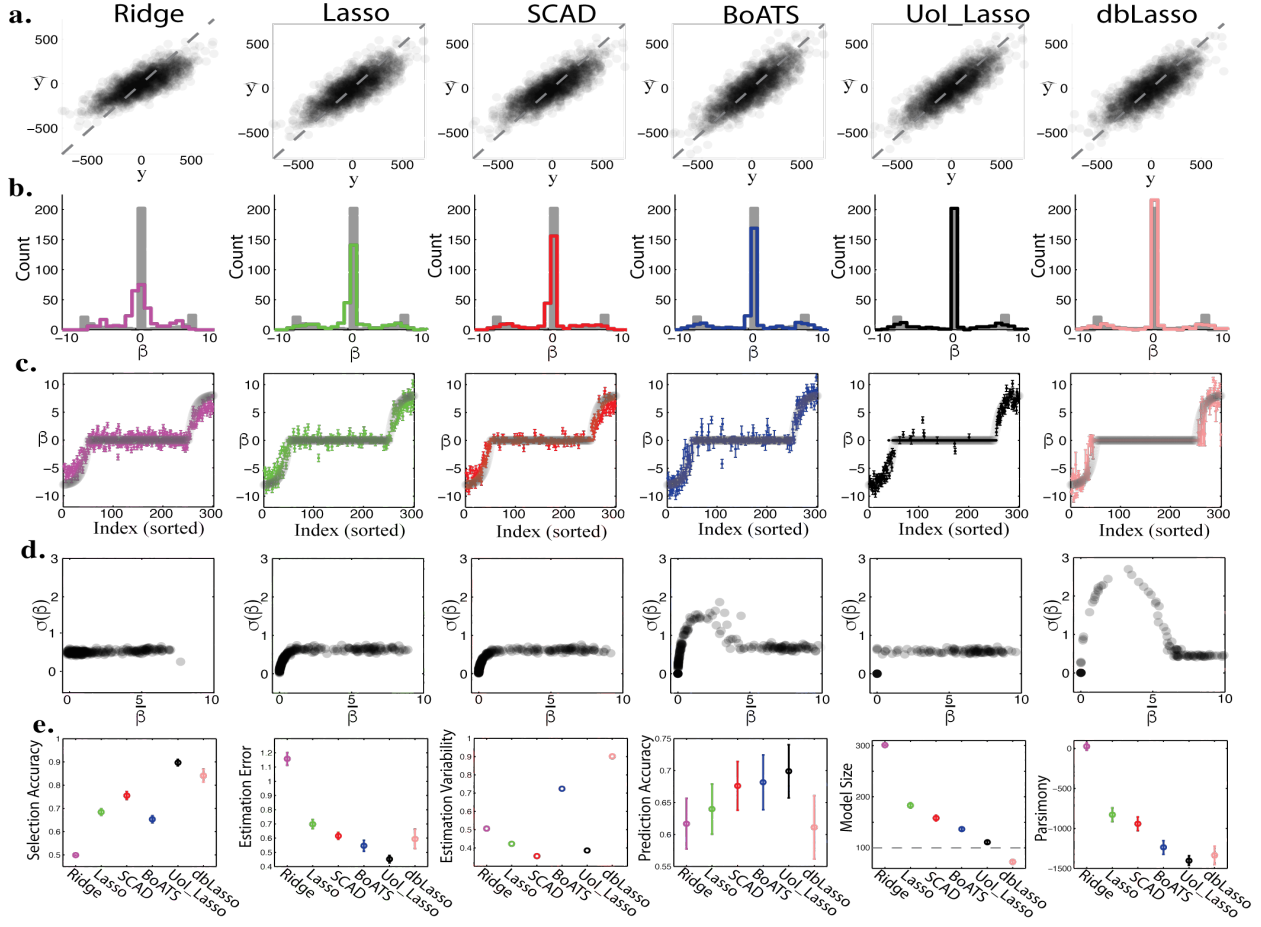


Figure 6: **Expanded range of observed results, in comparison with existing algorithms.**  $UoI_{Lasso}$  outperforms other methods.

Fig. 6(a) shows scatter plots of predicted vs. actual values of the observation variable on held-out data samples. Fig. 6(b) displays histograms of final model parameters (colors) overlaid on actual model parameters (grey). Fig. 6(c) plots the mean  $\pm$  s.d. of the estimate (colors) for each model parameter, ordered by the actual value of that parameter (actual values shown in grey). Fig. 6(d) shows the variability of the estimated values as a function of their magnitude. Fig. 6(e) quantifies a variety of properties of the results of each algorithm. Below, we summarize the results for each method, and we provide some intuition as to why these results are observed. This provides insight into the general superiority of the  $UoI_{Lasso}$  algorithm.

Ridge regression (purple) gave very weak model selection (i.e., few parameters equal to 0) and parameter estimates that were highly biased towards smaller values. This resulted in poor selection, estimation, and prediction accuracy, and the worst prediction parsimony (i.e., prediction accuracy

relative to number of non-zero model parameters). This is to be expected, as the  $L_2$  norm used by the algorithm is not a sparsity-inducing regularizer. Because the actual model in this case is quite sparse (only one-in-three parameters are non-zero), the relatively large value of the regularization parameter “shrinks” the values of all parameters towards zero, resulting in large bias.

The least angle shrinkage and selection operator (Lasso, green) is the industry standard method for regularized estimation of parameters in sparse models. It gave results that were much better than ridge regression for many metrics. However, it did only modestly well compared to the other algorithms tested here. This is to be expected, as the  $L_1$  norm used by Lasso is a sparsity inducing regularizer (i.e., unlike ridge, Lasso “shrinks” the values of all parameters towards zero to induce sparsity), but it imposes a Laplacian prior over the distribution of parameters (which in this example is known to be far from correct). That is, because the actual model in this example is both highly sparse and has many parameters with large magnitudes (counter to the Laplacian prior), Lasso resulted in only modest estimation error and prediction accuracy.

The Smoothly Clipped Absolute Deviation estimator (SCAD, red) is widely considered to be the state-of-the-art for regularized linear regression: for a given regularization strength, the magnitude of estimation shrinkage is larger for small values than for large values. This should result in both model selection and reduced bias in the estimation of large parameters. We found that SCAD had good data prediction accuracy, but intermediary selection accuracy and estimation error, and very low variability. It is worth noting here that SCAD has two main computational disadvantages compared to the rest of the algorithms presented here: it has a two-dimensional hyper-parameter space (though in practice, one of them is held constant), and (more seriously) it requires solving a non-convex optimization problem, making stability of solutions and scaling to large data sets less straightforward.

The Bootstrapped Adaptive Threshold Selection (BoATS) algorithm (blue) takes a very simple approach to model selection and estimation. First, it gets an initial estimate of all parameter values; then it sets all parameters below a threshold to zero and re-estimates the remaining parameters with bagged OLS; and then it optimizes the parameter threshold to maximize prediction accuracy (Fig. 6(a)). This has the attractive properties of setting many parameters exactly to zero so as to optimize prediction accuracy, and it gives nearly unbiased and accurate estimates of the remaining values (Fig. 6(c)). However, because of the hard thresholding combined with process noise, its estimates around the threshold are highly variable (Fig. 6(d)).

In a somewhat similar approach to BoATS, a recently proposed method to de-bias Lasso estimates and then use statistical tests (i.e., thresholds based on  $p$ -values) for model selection (debiased Lasso, pink) was overly aggressive, setting more values to zero than should be. This resulted in the worst data prediction accuracy, although it achieved good selection accuracy, estimation error and prediction parsimony. This can be understood because the selection of unbiased parameter estimates

according to an *a priori* arbitrary statistical criterion is done outside the context of optimizing prediction accuracy, and it sets many parameters exactly to zero.

$UoI_{Lasso}$  is designed to maximize prediction accuracy (Fig. 6(a), black) by first selecting the correct variables (Fig. 6(b), black), and then estimating their values with high accuracy (Fig. 6(c), black) and low variance (Fig. 6(d), black) with bagged OLS, which is nearly unbiased. It therefore offers the benefits of the strong selection algorithms (BoATS and debiased Lasso), but with the low variability of the structured regularizers (Lasso, SCAD), while simultaneously having accurate and nearly unbiased estimates. It also involves only calculations for convex optimizations, and so it scales very well.

To summarize these results, across all the algorithms we examined, we found that  $UoI_{Lasso}$  (black) generally resulted in the highest selection accuracy (Fig. 6(e), right), with parameter estimates with lowest error (Fig. 6(e), right-center) and competitive variance (Fig. 6(e), center-right). In addition, it led to the best prediction accuracy (Fig. 6(e), center-left), with a small number of model parameters (Fig. 6(e), left-center), giving best prediction parsimony (Fig. 6(e), left).

### A.5 $UoI_{Lasso}$ Outperforms Other Methods: Simulated Data with Different Parameter Distributions and Sparsity Levels

We further examined the generality of the superior performance of  $UoI_{Lasso}$  compared to other algorithms by simulating data generated by models with different underlying distributions. We varied both the distribution of the non-zero parameters (Fig. 7(a), black histograms) and the over-all sparsity of the model (Fig. 7(a), grey bar at zero). We kept constant: the number of non-zero parameters ( $k = 100$  for all); the noise ( $\sigma^2 = 0.2 \times \sum_j |\beta_j|$ ); and the number of samples ( $n$ ) relative to the total number of model parameters ( $p$ ) ( $n/p = 3$ ). We simulated data generated from four different distributions: exponentially decaying as a function of magnitude: roughly Laplacian (left); uniform (center left); exponentially increasing as a function of magnitude (center right); and clustered-positive (right). We varied the sparsity from 0 ( $p = 100$  parameters total) to 0.9 ( $p = 1000$  parameters total). Note that the number of samples in these simulations was different than for the example presented in Fig 2 and Fig. 6.

Generally speaking, across all distributions and levels of sparsity,  $UoI_{Lasso}$  generally had lowest estimation error (Fig. 7(b), black), highest prediction accuracy (Fig. 7(c), black), and lowest estimation variability (Fig. 7(e), black). The hard-thresholding procedures (BoATS and debiased Lasso) generally had the highest variability (Fig. 7(e), pink and blue). Across distributions, ridge regression (purple) and debiased Lasso (pink) had the strongest dependencies on sparsity. However, for all distributions, all methods except for  $UoI_{Lasso}$  exhibited systematic dependencies of selection accuracy on the degree of sparsity (Fig. 7(d)), while  $UoI_{Lasso}$  was nearly independent. Thus, for fixed  $B_1$  and  $B_2$ , the selection properties of  $UoI_{Lasso}$  depend only on the shape of the underlying

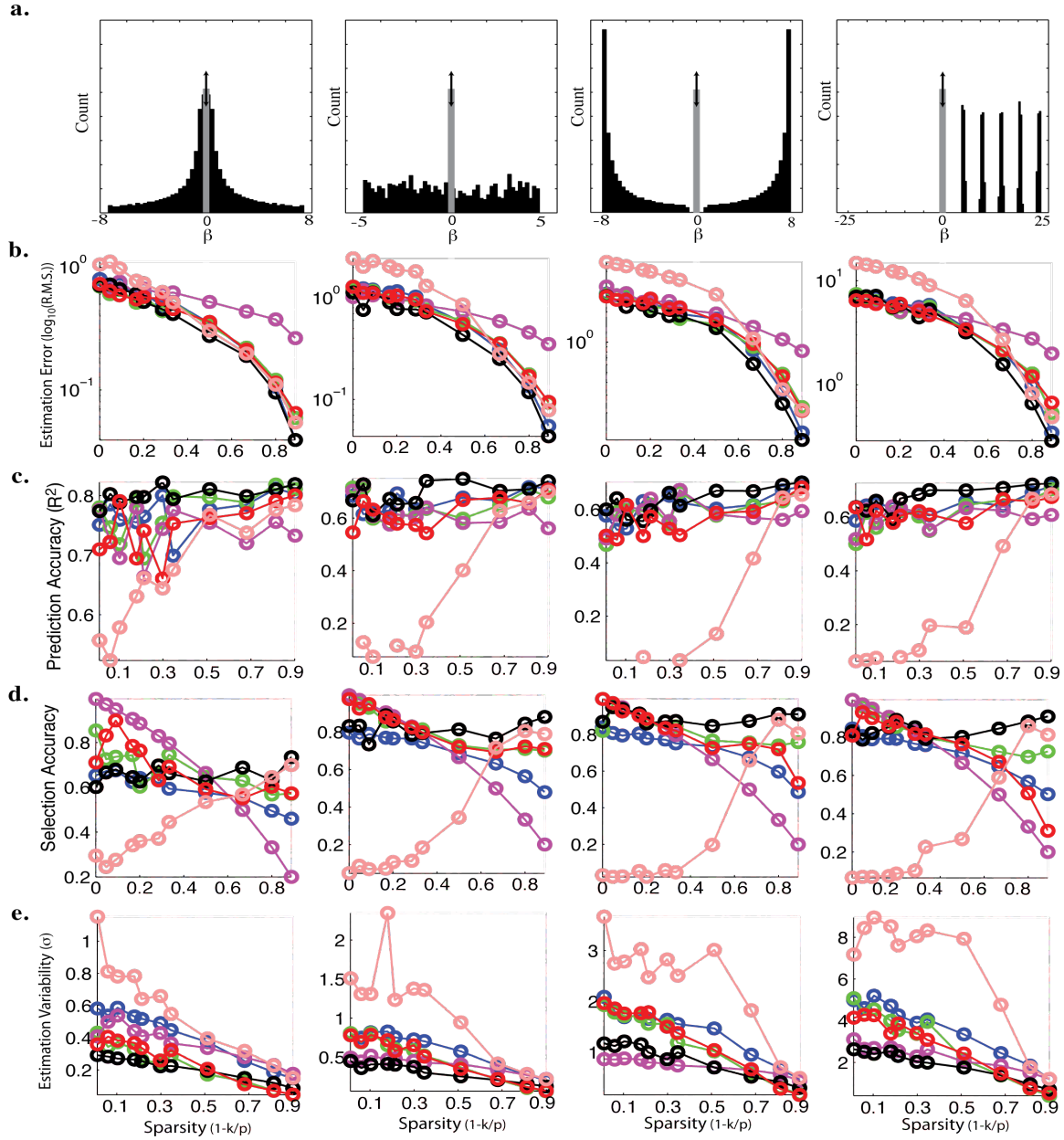


Figure 7: **Simulations across different parameter distributions and levels of sparsity.**  $UoI_{Lasso}$  outperforms other known methods. See the text for details and discussion.

non-zero parameter distribution and the amount of noise in the process, and not the overall degree of sparsity. This was a unique property of  $UoI_{Lasso}$ . The superior performance of  $UoI_{Lasso}$  on model estimation error and prediction accuracy despite reduced selection accuracies at low sparsities is due to the fact that the parameters that are getting set to zero are those that have very low magnitude and cannot be reliably estimated, given the amount of noise in the generating process.

### A.6 $UoI_{Lasso}$ Outperforms Other Methods: Simulated Data with Different Noise Magnitudes

To determine the robustness of  $UoI_{Lasso}$  to the magnitude of process noise, we examined the performance of the different methods as the magnitude of the process noise increased. Specifically, we varied the standard deviation of the additive Gaussian noise as a multiple of the summed weight magnitude ( $\sigma^2 = m \times \sum_j |\beta_j|$ ). The plots of Fig. 8(a)-(d) show results for data generated from the clustered model distribution (e.g., Fig. 7(a) right, sparsity:  $1 - k/p = 0.66$ ), for six values of the multiplicative factor  $m \in ([0 : 0.6])$ .

As expected, all algorithms performed very well when there was no noise, and most generally performed worse with increasing noise levels: estimation error and variability increased, prediction accuracy and support overlap decreased. Importantly, though,  $UoI_{Lasso}$  (black) generally performed as well as or better than the other algorithms, as the noise magnitude increased.

### A.7 $UoI_{L1Logistic}$ for Classification: Identifying Fewer Features without Loss of Prediction Accuracy

We have primarily demonstrated the power of the UoI method in the context of linear regression with the  $UoI_{Lasso}$  algorithm. However, the base UoI framework is much more general, and it can be applied to other regression problems, as well as other machine learning problems such as classification. To demonstrate this, we implemented a classification algorithm using logistic regression ( $UoI_{L1Logistic}$ ), and we compared it to  $L_1$ -Logistic regression on three diverse biomedical data sets from the UCI data repository. In the Dorothea data set, the goal is to find a small number of features that are predictive of whether a pharmaceutical compound is active (binds to target receptor) or inactive (is non-binding); in the Arcene data set, the problem of feature detection for prediction of cancer is presented, where mass spectrometry data indicating protein levels is used to separate healthy individual from those with cancer; and in the Parkinson’s Disease data set, the goal is to predict the stage of disease progression (a numerical score assigned by a clinician) from audio recordings of the patients speech. See Tables 1, 2, and 3 for a summary of our results. On all three of these data sets, in agreement with the results presented above on genetics, neuroscience, and synthetic data, we found that  $UoI_{L1Logistic}$  performed well with respect to both prediction and parsimony. In particular, it gave equivalent or better prediction accuracy, with many fewer

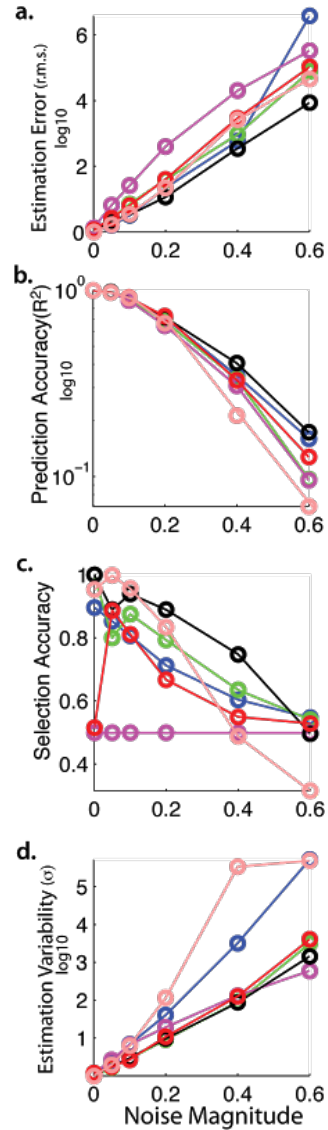


Figure 8: **Simulations across different noise magnitudes.**  $UoIL_{lasso}$  outperforms all other known methods. See the text for details and discussion.

parameters (3, 5, and 10 respectively), resulting in the best prediction parsimony.

Table 1:

Dorothea	Prediction Accuracy	Selection Ratio (PSR)	Parsimony (BIC)
$L_1$ -Logistic	93%	$53 \times 10^{-5}$	456
$UoI_{L1Logistic}$	93%	$3 \times 10^{-5}$	174

Table 2:

Arcene	Prediction Accuracy	Selection Ratio (PSR)	Parsimony (BIC)
$L_1$ -Logistic	66%	$59 \times 10^{-4}$	437
$UoI_{L1Logistic}$	66%	$5 \times 10^{-4}$	280

Table 3:

Parkinson's	Prediction Accuracy	Selection Ratio (PSR)	Parsimony (BIC)
$L_1$ -Logistic	65%	0.69	533
$UoI_{L1Logistic}$	68%	0.31	478

## A.8 $UoI_{CUR}$ for Matrix Decomposition

One of the popular dimensionality reduction methods used in many applications is the column subset selection problem (CSSP) [8], a variant of which is the so-called CUR matrix decomposition [16, 29]. Given a large data matrix  $A \in \mathbb{R}^{m \times n}$ , whose columns we wish to select, suppose  $V_k$  is the matrix consisting of the top  $k$  right singular vectors of  $A$ . Then, the leverage score of the  $i$ th column of  $A$  is given by

$$\ell_i = \frac{1}{k} \|V_k(i, :) \|^2_2, \quad (3)$$

i.e., by the norm of the  $i$ th row of  $V_k$ . In leverage score sampling, the columns of  $A$  are sampled using the probability distribution  $p_i = \min\{1, \ell_i\}$ , where  $\ell_i$  is given by Eqn. (3). Many popular methods for CSSP/CUR involve the use of this leverage score distribution as the importance sampling distribution with respect to which to sample columns [16, 8, 29]. (Importantly, while a naïve version of this algorithm is expensive, due to the computation of the SVD, the leverage scores of  $A$  can be well-approximated in the time it takes to perform a random projection on the matrix  $A$  [28, 15], and

the leverage score method has been applied to very large data sets [28, 22].) In this work, we show how the UoI framework can be adapted to the CSSP/CUR matrix decomposition problem.

The basic *UoICUR* algorithm is as follows. We consider the bootstrap resampling approach. We compute the different subsets of columns (and rows)  $C_i$  for the different bootstrap samples  $i = 1, \dots, B_1$ , and for different ranks  $k$  using leverage score sampling.

- **Intersection Step:** We then intersect the support (indices) of the subsets of columns (and rows)  $C_i$  over the bootstraps to obtain a smaller intersected subset  $\hat{C}^{(k)}$  (for different ranks  $k$ ). This intersection operation reduces the variance in sampling.
- **Union Step:** We then obtain a larger union set of columns by taking union of the intersected subsets  $\hat{C}^{(k)}$  over different ranks  $k$ .

As an illustration of the *UoICUR* algorithm, we have applied it to the analysis of genetics data. Analysis of gene expression DNA microarray data has become popular for studying a variety of biological processes [34]. In the microarray data, we have  $m$  genes (from  $m$  individuals, possibly from different populations) and a series of  $n$  arrays probe the genome-wide expression levels in  $n$  different samples, possibly under  $n$  different experimental conditions. Hence, the data from microarray experiments can be naturally represented as a matrix  $A \in \mathbb{R}^{m \times n}$ , where  $A_{ij}$  indicates whether the  $j$ th expression level exists for the  $i$ th gene. Typically, the matrix could have entries  $\{-1, 0, 1\}$ , indicating whether the expression exists ( $\pm 1$ ) or not (0), with the sign indicating the order of the sequence.

Article [34] used the CUR decomposition with a greedy column selection algorithm to select a subset of gene expressions or single nucleotide polymorphisms (SNPs) from a table of SNPs from different populations that capture the spectral information (or variations) of population. The subset of SNPs is called *tagging SNPs* (tSNPs). Here, we show how the *UoICUR* method can be applied in this application to select columns (and thus tSNPs from the table of SNPs) which characterize the extent to which major patterns of variation of the intrapopulation data are captured by a small number of tSNPs.

We use the same two datasets used in [34], namely the Yale dataset and the Hapmap datset. The Yale dataset<sup>1</sup> [33] contains a total of 248 SNPs from around 2000 unrelated individuals from 38 populations each (from around the world). We consider four genomic regions (*SORCS3, PAH, HOXB*, and *17q25*). The HapMap project<sup>2</sup> [21] (phase I) has released a public database of 1,000,000 SNP typed in different populations. From this database, we consider the data for the same four regions. Using the SNP table, an encoding matrix  $A$  is formed with entries  $\{-1, 0, 1\}$  indicating whether the expression exists ( $\pm 1$ ) or not (0), with the sign indicating the order of the sequence. See

---

<sup>1</sup><http://alfred.med.yale.edu/>

<sup>2</sup>[https://www.ncbi.nlm.nih.gov/variation/news/NCBI\\_retiring\\_HapMap/](https://www.ncbi.nlm.nih.gov/variation/news/NCBI_retiring_HapMap/)

Table 4: TaggingSNP:  $UoI_{CUR}$ , BasicCUR and GreedyCUR. See the text for details.

Data	Size	$c$	$UoI_{CUR}$	BasicCUR	GreedyCUR
Yaledataset/SORCS3	$1966 \times 53$	30	0.0096	0.0323	0.0062
Yaledataset/PAH	$1979 \times 32$	20	0.0165	0.0308	0.0165
Yaledataset/HOXB	$1953 \times 96$	36	0.0690	0.1369	0.0272
Yaledataset/17q25	$1962 \times 63$	35	0.0507	0.0895	0.0197
HapMap/SORCS3	$268 \times 307$	83	0.0023	0.0624	0.0023
HapMap/PAH	$266 \times 88$	42	0.0087	0.0130	0.0053
HapMap/HOXB	$269 \times 571$	57	0.0840	0.1696	0.0211
HapMap/17q25	$265 \times 370$	80	0.0421	0.1819	0.0162

supplementary material of [34] for details on this encoding. We obtained such encoded matrices from <http://www.asifj.org/>, as made available online by the authors of [34].

Table 4 lists the errors obtained from the three different methods, namely,  $UoI_{CUR}$ , BasicCUR and GreedyCUR [34] for different populations. The error reported is given by  $nnz(\hat{A} - A)/nnz(A)$ , where  $A$  is the input encoding matrix,  $C$  is the sampled/coarsened matrix,  $\hat{A} = CC^\dagger A$ , is the projection of  $A$  onto  $C$  and  $nnz(A)$  is the number of elements in  $A$ . The GreedyCUR algorithm considers each column of the matrix sequentially, projects the remaining columns onto the considered column, and chooses the column that gave least error (where error is defined above). The algorithm then repeats the procedure to select the next column, and so on. This algorithm is very expensive, but it performs very well in practice. We observe that the  $UoI_{CUR}$  algorithm performs better than BasicCUR, and the performance is comparable with the unscaleable GreedyCUR algorithm in many cases.

## A.9 Additional Discussion

It is common in many machine learning and data analysis methods to have either an implicit or explicit tradeoff between interpretability and prediction accuracy [2]. For example, in the context of unsupervised dimensionality reduction, CUR decompositions are low-rank approximations that are expressed in terms of a small number of actual rows and columns of the data matrix (i.e., actual data elements). It is known that they are provably only slightly worse in terms of variance reconstruction than the eigenvectors provided by PCA, but since they correspond to actual data elements, they are more easily interpretable in terms of the biological processes generating the data [29]. In a similar manner, in the context of supervised learning, UoI selects features and estimates parameters to optimize prediction accuracy while maintaining parsimony, resulting in interpretable models without

substantially sacrificing prediction accuracy. Looking forward, the basic UoI framework can be applied to other algorithms to explore this trade-off more generally.

From a statistical perspective, we have illustrated four key properties of  $UoI_{Lasso}$ : control of false positive and false negative selection errors, and improved model selection consistency and data prediction accuracy. On both real and synthetic data, we observed generally improved prediction accuracy on held-out data, despite fewer parameters, a phenomenon we attribute to better up-front model selection reducing over-fitting on the training data. Importantly, when the feature space is dense,  $UoI_{Lasso}$  has no systemic disadvantage relative to other methods (nor does it offer any advantage). It is common in many scientific fields to calculate a “score” (such as False Discovery Rate, FDR), independently for each feature, and then select features that exceed a (statistical) threshold, e.g., a p-value. This approach has several potential disadvantages. In particular, because of the independent (i.e., pair-wise) nature of some of these analysis, it is not possible to disambiguate features that uniquely contribute to a response, as opposed to simply co-vary with the causal features. Dependence between features can severely challenge most existing methods. Furthermore, even if estimation is done across all features simultaneously, selection is often done after estimation, and not in the context of response prediction (e.g., debiased Lasso). Additionally, the selection of a threshold (e.g.,  $p < 0.05$ , multiple comparisons corrected) is often *a priori* arbitrary with respect to response prediction. Likewise, in the generation of genetic and brain networks, the underlying graphs need to be estimated from data. In practice, experimenters often apply a *post hoc* threshold to the distribution of edge weights (often, marginal correlation) outside the context of optimizing prediction accuracy (the objective function). These *ad hoc* processes challenge rigorous mathematical analysis; they can dramatically alter the structure of empirical results; and they are likely a major source of error in downstream scientific conclusions. In contrast, using the UoI approach for model selection and model estimation to optimize prediction suggests a potentially general, normative framework for overcoming these and other related algorithmic-statistical issues in a scalable way.

From an algorithmic perspective,  $UoI_{Lasso}$  efficiently constructs a family of model supports by combining randomized data resampling with a range of regularization hyperparameters, imbuing  $UoI_{Lasso}$  with a high degree of parallelization, making it a natural fit for modern distributed computing platforms. We provide open-source implementations of  $UoI_{Lasso}$  in Matlab, R, and Python to make it as broadly and easily accessible as possible. Additionally, we provide versions of  $UoI_{Lasso}$  in Python that use either OpenMP or Spark for efficient implementation on a variety of distributed computing platforms [19]. The current computing bottleneck in  $UoI_{Lasso}$  for application to massive data sets is the calculations involved in solving the core Lasso/OLS problem, suggesting that recent work in distributed convex optimization or sampling-based techniques from randomized linear algebra may lead to still further benefits.

From the perspective of scalable, interpretable, scientific data analysis, the modular structure of

UoI is particularly powerful, as it allows for a diversity of methods to be used, making it both general and flexible. In the context of linear regression, use of BoLasso for model selection and ordinary least squares (OLS) for model estimation resulted in the *UoILasso* algorithm primarily studied here; but the UoI framework can accommodate other base methods such as stability selection [32], SCAD [17], debiased Lasso [26], or other specialized, problem specific methods. Alternatively, in the context of classification, support vector machines or other classifiers could have been used [12]. More generally, we see no reason why the UoI framework could not be extended to more complex statistical models, such as random forests [10], auto-regressive models, and canonical correlation analysis [25]. Relatedly, while data analysis methods in science are often heavily tailored to a specific domain, the UoI method is a modality-agnostic data analytic method, and the problems for which we have demonstrated its utility (regression and classification) are ubiquitous across data domains in science and industry, e.g., material science and climate science, in addition to neuroscience and genetics. Therefore, there is every reason to believe that UoI and related methods could enhance interpretable scientific machine learning in other scientific fields in gigabyte, terabyte, and petabyte sized data sets that are increasingly common.